JACS
JOURNAL OF THE AMERICAN CHEMICAL SOCIETY
Communication
pubs.acs.org/JACS

Imaging of Nonuniform Motion of Single DNA Molecules Reveals the Kinetics of Varying-Field Isotachophoresis

Shengquan Liu, Bailin Zhao, Dapeng Zhang, Cuiping Li, and Hailin Wang*

State Key Laboratory of Environmental Chemistry and Ecotoxicology, Research Center for Eco-Environmental Sciences, Chinese Academy of Sciences, Beijing 100085, P. R. China

Supporting Information

ABSTRACT: The nonuniform motion of charged species in a varying electric field may provide unique separation and focusing power for chemical, biochemical, and nanoscale studies. We imaged in real time the nonuniform motion of single DNA molecules under varying-field isotachophoresis (ITP) conditions. From the trajectories of single molecules, we obtained the time- and position-dependent electric field strength (E) and revealed the behavior of adaption barriers within electro-osmotic flow (EOF)-driven and EOF-independent ITP. We found that the initial terminating electrolyte zone of constant E is split into two zones: a highly adapted high-E zone and a low-E zone of gradually adapting electric field. The formation of the two unique zones is associated with the rate-limiting mass transfer barrier in EOF-driven ITP. As a result of the unique E distribution, DNA molecules first slow to a stop and then rapidly move backward to the leading electrolyte/terminating electrolyte boundary. This provides a novel mechanism for selective focusing of target molecules in dilute solutions of large volume. We show that the ITP focusing can improve the detection of single DNA molecules (limit of detection = 4×10^{-17} mol/L), which are stochastically distributed at extremely low concentrations. The ITP strategy focuses individual molecules into a small volume that is matched with the focal point of single-molecule imaging.

The behaviors of charged species under a uniform or nonuniform electric field provide a foundation for various electrophoresis applications in chemistry, physics, life sciences, and emerging nanotechnologies.[1] The motion of charged species is well-described in a uniform electric field but not in a nonuniform electric field. Rationally designed nonuniform electric fields offer extraordinary capabilities for resolving large DNA molecules[2] and preconcentrating various analytes,[3] but monitoring the nonuniform motion of charged species in a nonuniform electric field is technically challenging.[4]

In this work, using advanced single molecule imaging (SMI),[5] we for the first time examined the nonuniform motion of single DNA molecules in response to changes in the electric field. Our study was conducted using capillary isotachophoresis (cITP).[3] Individual DNA molecules passing the detection window were consecutively imaged in real time at 50 ms intervals. Since the DNA migration velocity is directly proportional to the applied electric field strength (E), imaging the movement of DNA allows the distribution of E throughout the capillary to be determined. This approach provided insights into the kinetics of varying-field ITP and enabled us to develop a strategy to focus and detect single DNA molecules.

A simplified ITP system (Scheme 1) consists of a leading electrolyte (LE) and a terminating electrolyte (TE). Under constant E throughout the separation compartment, the fast-moving LE would leave a gap ahead of the slow-moving TE with no ions to conduct electricity;[6] therefore, the LE and TE must migrate at the same velocity (Scheme 1). The velocity (v) is equal to the product of E and the electrophoretic mobility (μ):

$$v_{TE} = v_{LE} = \mu E \quad (1)$$

Therefore, E must adapt to the electrophoretic mobility in each zone:[6] the LE zone (high μ) must have a low E, and the TE zone (low μ) must have a high E (Scheme 1). Current literature commonly assumes that the adaption of E is fast and is not the rate-limiting step. However, the actual adaption kinetics of ITP has not been studied to date. Moreover, it is not clear how electro-osmotic flow (EOF) affects the dynamics of ITP.

We first tested the dynamics of cITP in the presence of EOF. A fused silica capillary was fully filled with the TE and calf thymus (ct) DNA (4.5 pM), and then the LE was continuously introduced into the capillary (Figure 1A). Since the concentration of ctDNA was 10 orders of magnitude lower than that of the electrolytes (~10 mM), the presence of ctDNA in the capillary did not significantly affect the tested electric field. To visualize the ctDNA molecules, we stained them with excess YOYO-1 (10 nM).[7] We imaged individual stained DNA molecules repeatedly. Each frame in Figure 1B corresponds to

Scheme 1. E Distribution in Anionic ITP[a]

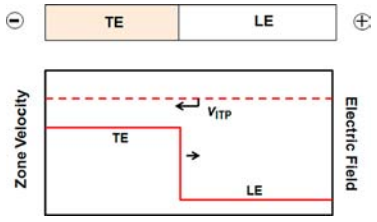

[a]At steady state, the LE zone (high μ) and TE zone (low μ) must migrate at the same velocity and therefore adapt to generate low E and high E, respectively.

Received: January 5, 2013
Published: March 12, 2013

dx.doi.org/10.1021/ja400126b | J. Am. Chem. Soc. 2013, 135, 4644−4647

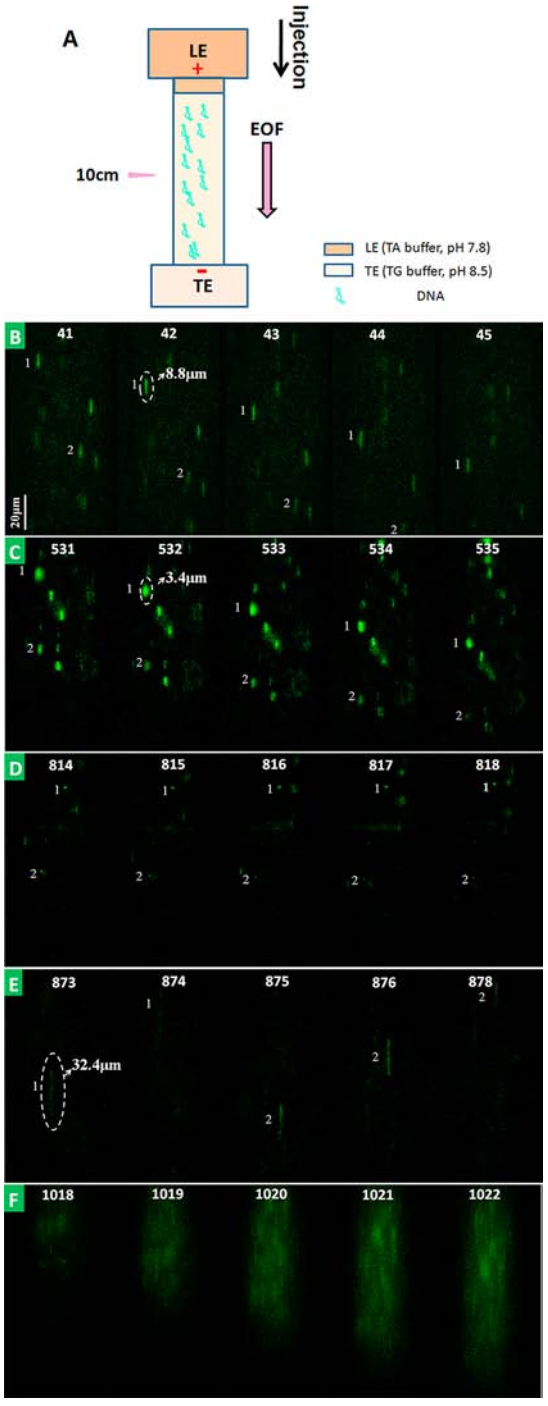

Figure 1. (A) Schematic illustration of the ITP system, in which 0.5× Tris-glycine (TG) buffer (pH 8.5) was used as the TE and 2× Tris-acetic acid (TA) buffer (pH 7.8) as the LE. (B–D) Imaging of fluorescently labeled DNA molecules in a capillary: (B) frames 41–45 (13.5 to 14.8 s); (C) frames 531–535 (2 min 55 s to 2 min 56.4 s); (D) frames 814–818 (4 min 28.2 s to 4 min 29.4 s); (E) frames 873–877 (4 min 48 s to 4 min 49.2 s); (F) frames 1018–1022 (5 min 35.9 s to 5 min 37.2 s).

an integrated measurement of the fluorescence over 50 ms. Therefore, each line represents the migration of a DNA molecule during a 50 ms period. The lengths of these lines reflect the real-time migration velocities of the DNA molecules.

Figure 1B–F and the video in the Supporting Information (SI) show the changes in migration of DNA molecules over time. Frames 41–45 (Figure 1B), corresponding to the time interval from 13.5 to 14.8 s, show that the average trajectory length of single DNA molecules was 8.8 μm, while frames 531–535 (Figure 1C) show an average trajectory length of 3.7 μm, indicating the nonuniform velocity of DNA molecules under ITP. In frames 814–818 (Figure 1D), the images of the individual DNA molecules are circular points, and their axial positions do not shift in the consecutive frames, suggesting that the DNA molecules stopped migrating temporarily (7.8 s). The DNA molecules then rapidly migrated backward (toward the positive end), as shown by the long trajectories (32.4 μm) and the change in the direction of motion (Figure 1E; compare molecule 1 in frames 874 vs 873 and molecule 2 in frames 876 vs 875). Finally, when the DNA molecules reached the LE/TE boundary (Figure 1F, frames 1018–1022), they again moved forward (toward the negative end). In the ITP process, DNA molecules were continuously focused at the LE/TE boundary. The bright spot in the frames in Figure 1F results from the focusing of many DNA molecules at the LE/TE boundary in the capillary.

We measured the velocities of the DNA molecules from the lengths of the trajectories (streak method) and the positional shifts (multiframe method) and obtained identical velocity–time curves from the two methods (Figure S1). By setting the imaging window at different axial positions of the capillary, we measured the DNA migration velocity over time at three distances from the anode (Figure 2A). Regardless of the position of the imaging

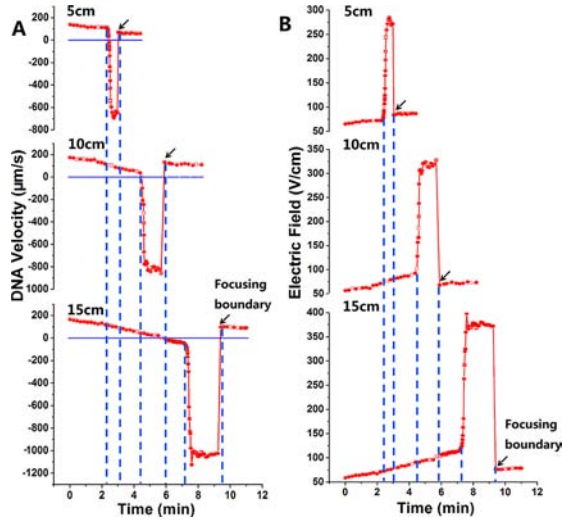

Figure 2. (A) DNA migration velocity and (B) electric field strength as functions of migration time in EOF-driven ITP. The images were recorded at 5, 10, or 15 cm from the positive end (inlet) of the 20 cm capillary. Mean velocities and standard deviations were estimated from triplicate analysis.

window, the velocity–time curve has three sections (Figure 2A). The initial segment shows a gradual decrease in the DNA migration velocity. This is followed by a rapid change to DNA migration in the negative direction, with velocities having magnitudes as high as 600–1000 μm/s. The last segment displays a constant velocity of DNA molecules migrating in the original (positive) direction (i.e., from the anode to the cathode under the influence of EOF). The three sections in Figure 2A are consistent with the three stages of motion visualized in Figure 1B–F): slowing to stop, moving backward, and moving steadily forward. For example, when the imaging window was located at 10 cm, DNA molecules with an initial velocity of 174 μm/s

dx.doi.org/10.1021/ja400126b | J. Am. Chem. Soc. 2013, 135, 4644–4647

slowed to a stop at 4.51 min and then changed direction, rapidly moving backward with a sharply increased velocity of 856 μm/s (4.51−5.72 min). After the DNA molecules arrived and were focused at the LE/TE boundary, they moved forward with the boundary at a velocity of ~120 μm/s.

Since the migration velocity is related to E, μ, and the EOF velocity (v_{EOF}) (see the SI), we could estimate E once μ and v_{EOF} were known. Thus, we first measured v_{EOF} by using neutral markers and found that it was almost constant throughout the tested ITP process (Figure S2). We then measured μ for the DNA molecules. At a constant E of 100 V/cm, the measured value was 3.88×10^{-4} cm^2 V^{-1} s^{-1}. On the basis of velocity−time curves and the v_{EOF} and μ values, we obtained electric field−time curves that exhibit three discrete zones: a high-E zone flanked by two low-E zones (Figure 2B).

This phenomenon has not been reported previously. How do three distinct E zones form in a system containing only two electrolytes (the LE and the TE)? Since DNA molecules are focused at the TE/LE boundary in ITP,[6] the LE/TE boundary can be visualized by screening of SMI frames (e.g., Figure 1F). Moreover, the TE zone migrates out earlier than the LE zone in EOF-driven ITP. Hence, the locations of the LE and TE zones can be exactly visualized. From the view of the focusing boundary (i.e., the TE/LE boundary), indicated by the arrows in Figure 2B, we conclude that the TE zone that initially fills the entire capillary is quickly split into two new TE zones: a high-E zone adjacent to the LE and a low-E zone distant from the LE. Therefore, we propose a three-zone model to describe the EOF-driven ITP process (Figure S3A).

The proposed three-zone model for the EOF-driven ITP is further supported by the data obtained from the three different imaging positions (Figure 2). If there were only two zones, the high-E TE zone would have been partly overlapped when monitored at any axial position. This was not the case, as we did not observe any overlapping of the high-E zones in the electric field−time curves at the three imaging positions (Figure 2B).

Additional insights into the basis for the three observed E zones under the EOF-driven ITP conditions can be gained from the following theoretical treatment. The regulation of the TE zones should obey Ohm's law and current continuity, which are generally applicable to any electrophoretic conditions.[8] Thus, we can directly apply Ohm's law:

$$E\delta = J \tag{2}$$

where J is the current density at the given location in a resistive electrolyte and δ is the conductivity, given by

$$\delta = \sum_i C_i|\mu_i|F \tag{3}$$

in which C_i is the concentration of the ith ion and F is the Faraday constant. With constant cross-sectional area, J is constant at any axial position through the capillary. Combining eqs 2 and 3 yields J as a function of E and the C_i:

$$J = E\sum_i C_i|\mu_i|F \tag{4}$$

Evidently, E is inversely proportional to the ion concentrations when J is constant. In the three-zone E distribution in the EOF-driven ITP (Figure 2B and Figure S3A), the new high-E TE zone has E values 6 times higher than the initial value. Thus, according to eq 4, the new high-E TE zone in the EOF-driven ITP should have a much lower ion concentration than the initial TE zone (with a 6-fold lower E value) and is a highly adapted zone. Indeed, a dilute TE zone was observed between the undiluted TE zone and the LE zone (Figure S4). The remainder of the TE zone exhibits only a gradual increase in E, which is not as high as in the highly adapted TE zone (Figure 2B). However, when more LE is injected into the capillary, this low-E zone is gradually converted to a new highly adapted zone of increasing E.

As discussed above, the formation of a highly adapted TE zone with a greatly reduced ion concentration is critical for the generation of a high electric field. In EOF-driven ITP, the TE fills the capillary before electrokinetic injection of the LE, and the formation of the highly adapted TE zone requires a large-scale mass transfer to remove most of the TE from the existing zone. Therefore, the E adaptation is a rate-limited step in EOF-driven ITP because of the large-scale mass transfer in the TE zone.

To support the above conclusion, we determined the DNA migration velocity when the EOF was suppressed. In these experiments, the neutral capillary was first fully filled with LE, and then TE was electrokinetically injected into the capillary by applying power at high voltage (Figure 3A). We suspected that

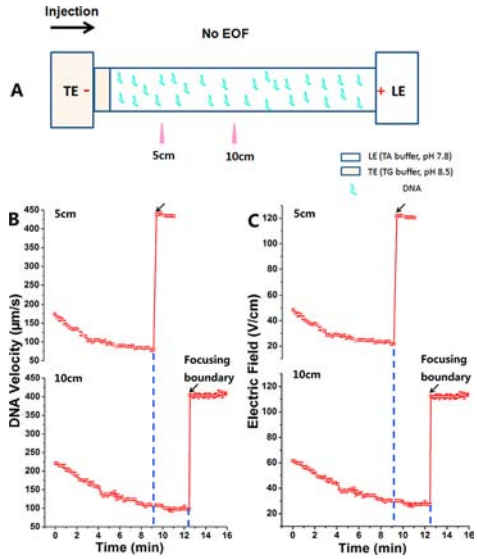

Figure 3. (A) Schematic of the EOF-suppressed ITP experiment. (B) DNA migration velocity and (C) electric field strength as functions of migration time in EOF-suppressed ITP. Images were recorded 5 or 10 cm from the negative end (inlet) of the 20 cm capillary. Mean velocities and standard deviations were estimated from triplicate analysis.

the electrokinetic injection of the TE would facilitate rapid mass transfer to form a diluted TE zone without splitting of the initial TE zone. Indeed, we observed only two zones in the EOF-suppressed ITP: a low-E LE zone and a high-E TE zone (Figure 3C). This observation was independent of the monitoring position (Figure 3B,C) and consistent with the traditional theory of ITP (Scheme 1).[6] Therefore, a two-zone model is sufficient to describe the EOF-independent ITP (Figure S3B).

The formation of two TE zones by splitting of the initial TE zone in EOF-driven ITP may provide a novel means for selective focusing of target molecules in dilute solutions of large volume, which may facilitate DNA SMI by squeezing the analytes from a large volume (μL) into the LE/TE boundary, which may have a small, SMI-matched volume (pL). Interestingly, 2−3 DNA molecules at a concentration of 4×10^{-17} M could be detected at the focusing boundary using the developed ITP focusing approach (Figure 4). In contrast, no DNA molecules could be observed without ITP focusing (data not shown). At such an

dx.doi.org/10.1021/ja400126b | J. Am. Chem. Soc. 2013, 135, 4644−4647

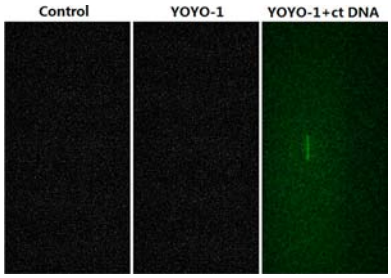

Figure 4. Sensitive detection of YOYO-1-stained ctDNA in the EOF-driven ITP system. The imaging window was set at 15 cm/20 cm. ctDNA at a concentration of 4×10^{-17} M stained with 1 nM YOYO-1 was filled into the whole capillary (right). Two negative controls were used: no YOYO-1 or DNA was injected (left) and 1 nM YOYO-1 but no DNA was injected (middle).

extremely low concentration, the presence of DNA molecules in the detection volume (~25 pL) is a stochastic event, even though single-molecule detection is thought to be an extremity of analytical technologies. The probability of the presence of one DNA molecule is estimated to be only $\sim 6 \times 10^{-4}$. Therefore, no DNA molecules could be detected even by SMI when no focusing was employed.

In traditional theory, ITP can be achieved simply by placing ionic analytes between the leading and terminating ions,[6b] which have the highest and lowest electrophoretic mobilities in the involved system, respectively. However, as demonstrated by this work, an adaptation barrier can be observed in EOF-driven ITP. In ITP, the formation of a diluted TE zone with a high *E*, which is essential for ITP separation and focusing, is determined by the mass transfer barrier of the TE. In EOF-independent ITP, the prior-filled LE zone is gradually adapted to produce a low *E*, which can be explained with the traditional two-zone model. In the presence of EOF, to achieve possible ITP separation and focusing, the TE should be filled in the capillary before the LE. This changes the kinetics of ITP and produces a barrier for the adaptation of the electric field to the lately injected LE. Therefore, EOF-driven ITP can be explained only by using a three-zone model, and the corresponding ITP theory should be updated. This is the first plausible report of the three-zone distribution of *E* in the EOF-driven ITP process.

Our findings not only clarify the adaptation barriers for ITP but also provide a foundation for potential applications, including large-volume focusing and selective injection of charged species. As demonstrated in this work, large-volume focusing may improve the detection of single molecules, which is a stochastic event at extremely low concentrations, by squeezing the analytes from a large volume into a small, SMI-matched volume. On the other hand, the observed backward movement of DNA molecules may indicate the capacity to inject anionic species from the capillary end having negative polarity, providing a new selective injection module.

The clarification of the dynamic ITP process will benefit from our approach for quantitative profiling of nonuniform DNA motion and the associated electric field. This work demonstrates the novel application of SMI to investigate nonuniform motion and monitor changes in *E*, opening a new way to probe the motion of biomolecules in a varying electric field.

In summary, we have extended the single molecule imaging technique to study visually and quantitatively the separation and focusing of isotachophoresis and provide new insights into the mechanism and kinetics of ITP. On the basis of our mechanistic study, we propose a three-zone model to describe EOF-driven ITP and demonstrate its practical application for improving DNA analysis and detection of single DNA molecules.

■ ASSOCIATED CONTENT

Supporting Information

Experimental details and supporting data. This material is available free of charge via the Internet at http://pubs.acs.org.

■ AUTHOR INFORMATION

Corresponding Author

hlwang@rcees.ac.cn

Notes

The authors declare no competing financial interest.

■ ACKNOWLEDGMENTS

This work was supported by grants from the National Basic Research Program of China (2011CB936001, 2009CB421065, and 2011YQ060084) and the National Natural Science Foundation of China (21077129, 20890112, and 21125523).

■ REFERENCES

(1) (a) Wegman, D. W.; Krylov, S. N. *Angew. Chem., Int. Ed.* **2011**, *50*, 10335. (b) Zhang, H.; Li, X.-F.; Le, X. C. *J. Am. Chem. Soc.* **2007**, *130*, 34. (c) Mendonsa, S. D.; Bowser, M. T. *J. Am. Chem. Soc.* **2004**, *126*, 20. (d) Wojcik, R.; Vannatta, M.; Dovichi, N. J. *Anal. Chem.* **2010**, *82*, 1564. (e) Wang, H.; Lu, M.; Tang, M.-S.; Houten, B. V.; Alexander Ross, J. B.; Weinfeld, M.; Le, X. C. *Proc. Natl. Acad. Sci. U.S.A.* **2009**, *106*, 12849. (f) Roman, G. T.; Wang, M.; Shultz, K. N.; Jennings, C.; Kennedy, R. T. *Anal. Chem.* **2008**, *80*, 8231. (g) Zhao, S. S.; Zhong, X.; Tie, C.; Chen, D. D. Y. *Proteomics* **2012**, *12*, 2991. (h) Zhang, D. P.; Lu, M.; Wang, H. *J. Am. Chem. Soc.* **2011**, *133*, 9188.

(2) Schwartz, D. C.; Cantor, C. R. *Cell* **1984**, *37*, 67.

(3) (a) Shackman, J. G.; Ross, D. *Anal. Chem.* **2007**, *79*, 6641. (b) Wang, Z.; Lu, M.; Wang, X.; Yin, R.; Song, Y.; Le, X. C.; Wang, H. *Anal. Chem.* **2009**, *81*, 10285. (c) Gebauer, P.; Malá, Z.; Boček, P. *Electrophoresis* **2011**, *32*, 83. (d) Hirokawa, T.; Takayama, Y.; Arai, A.; Xu, Z. Q. *Electrophoresis* **2008**, *29*, 1829. (e) Britz-McKibbin, P.; Bebault, G. M.; Chen, D. D. Y. *Anal. Chem.* **2000**, *72*, 1729.

(4) (a) Johansson, J.; Witte, D. T.; Larsson, M.; Nilsson, S. *Anal. Chem.* **1996**, *68*, 2766. (b) Chambers, R. D.; Santiago, J. G. *Anal. Chem.* **2009**, *81*, 3022. (c) Khurana, T. K.; Santiago, J. G. *Anal. Chem.* **2008**, *80*, 279.

(5) (a) Moerner, W. E. *Proc. Natl. Acad. Sci. U.S.A.* **2007**, *104*, 12596. (b) Forget, A. L.; Kowalczykowski, S. C. *Nature* **2012**, *482*, 423. (c) Gorman, J.; Wang, F.; Redding, S.; Plys, A. J.; Fazio, T.; Wind, S.; Alani, E. E.; Greene, E. C. *Proc. Natl. Acad. Sci. U.S.A.* **2012**, *109*, E3074. (d) Elenko, M. P.; Szostak, J. W.; Oijen, A. M. V. *J. Am. Chem. Soc.* **2009**, *131*, 9866. (e) Chen, D. Y.; Dovichi, N. J. *Anal. Chem.* **1996**, *68*, 690. (f) Anazawa, T.; Matsunaga, H.; Yeung, E. S. *Anal. Chem.* **2002**, *74*, 5033.

(6) (a) *Handbook of Capillary Electrophoresis*; Landers, J. P., Ed.; CRC Press: Boca Raton, FL, 1994. (b) Holloway, C. J.; Trautschold, I. *Fresenius' Z. Anal. Chem.* **1982**, *311*, 81.

(7) Marino, M. A.; Devaney, J. M.; Davis, P. A.; Smith, J. K.; Girard, J. E. *Anal. Chem.* **1998**, *70*, 4514.

(8) (a) Beckers, J. L.; Everaerts, F. M.; Ackermans, M. T. *J. Chromatogr.* **1991**, *537*, 429. (b) Thormann, W. *J. Chromatogr.* **1990**, *516*, 211. (c) Beckers, J. L.; Everaerts, F. M. *J. Chromatogr.* **1990**, *508*, 3. (d) Beckers, J. L.; Boček, P. *Electrophoresis* **2000**, *21*, 2747.